



Strathprints Institutional Repository

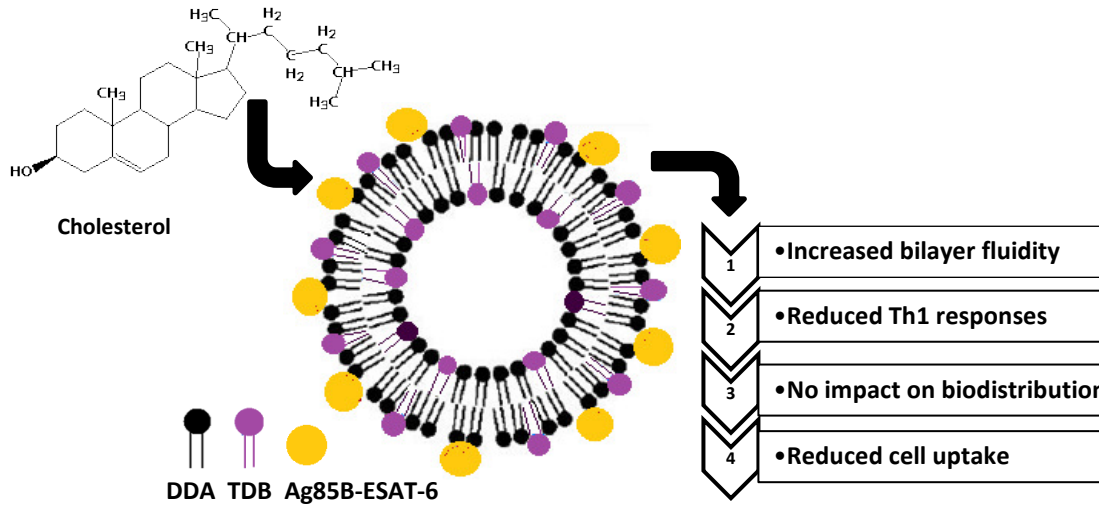
Kaur, Randip and Henriksen-Lacey, Malou and Wilkhu, Jitinder and Devitt, Andrew and Christensen, Dennis and Perrie, Yvonne (2014) Effect of incorporating cholesterol into DDA:TDB liposomal adjuvants on bilayer properties, biodistribution, and immune responses. *Molecular Pharmaceutics*, 11 (1). pp. 197-207. ISSN 1543-8384 , <http://dx.doi.org/10.1021/mp400372j>

This version is available at <http://strathprints.strath.ac.uk/56820/>

Strathprints is designed to allow users to access the research output of the University of Strathclyde. Unless otherwise explicitly stated on the manuscript, Copyright © and Moral Rights for the papers on this site are retained by the individual authors and/or other copyright owners. Please check the manuscript for details of any other licences that may have been applied. You may not engage in further distribution of the material for any profitmaking activities or any commercial gain. You may freely distribute both the url (<http://strathprints.strath.ac.uk/>) and the content of this paper for research or private study, educational, or not-for-profit purposes without prior permission or charge.

Any correspondence concerning this service should be sent to Strathprints administrator: strathprints@strath.ac.uk

Graphical Abstract:



1 **Title:** The effect of incorporating cholesterol into DDA:TDB liposomal adjuvants on
2 bilayer properties, biodistribution and immune responses.

3 **Authors:** Randip Kaur^{1#}, Malou Henriksen-Lacey^{2#}, Jitinder Wilkhu¹, Andrew Devitt^{1,3},
4 Dennis Christensen⁴, Yvonne Perrie^{1,3*}

5

6

7 ¹Medicines Research Unit, School of Life and Health Sciences, Aston University,
8 Birmingham, UK. B4 7ET.

9 ²CICbiomaGUNE, PARQUE TECNOLÓGICO DE SAN SEBASTIÁN, Edificio Empresarial
10 "C". Paseo Miramon 182, GUIPÚZCOA, SPAIN.

11 ³Aston Research Centre for Healthy Ageing (ARCHA), Aston University, Birmingham, UK.
12 B4 7ET.

13

14 ⁴Department of Infectious Disease Immunology, Statens Serum Institut, DK-2300
15 Copenhagen, Denmark.

16 #these authors contributed equally to this work

17

18 **Date of manuscript: revised 1st Oct 2013**

19

20

21

22 *Correspondence: Professor Yvonne Perrie
23 Medicines Research Unit
24 School of Life and Health Sciences
25 Aston University, Birmingham, UK. B4 7ET.
26 Tel: +44 (0) 121 204 3991
27 Fax: +44 (0) 121 359 0733
28 E-mail: y.perrie@aston.ac.uk
29

30

31 **Abstract**

32 Cholesterol is an abundant component of mammalian cell membranes and has been
33 extensively studied as an artificial membrane stabiliser in a wide range of phospholipid
34 liposome systems. In this study, the aim was to investigate the role of cholesterol in cationic
35 liposomal adjuvant system based on dimethyldioctadecylammonium (DDA) and trehalose
36 6,6'-dibehenate (TDB) which has been shown as a strong adjuvant system for vaccines
37 against a wide range of diseases. Packaging of cholesterol within DDA:TDB liposomes was
38 investigated using differential scanning calorimetry and surface pressure-area isotherms of
39 lipid monolayers; incorporation of cholesterol into liposomal membranes promoted the
40 formation of a liquid-condensed monolayer and removed the main phase transition
41 temperature of the system, resulting in an increased bilayer fluidity and reduced antigen
42 retention *in vitro*. *In vivo* biodistribution studies found that this increase in membrane fluidity
43 did not alter deposition of liposomes and antigen at the site of injection. In terms of immune
44 responses, early (12 days after immunisation) IgG responses were reduced by inclusion of
45 cholesterol, thereafter there were no differences in antibody (IgG, IgG1, IgG2b) responses
46 promoted by DDA:TDB liposomes with and without cholesterol. However, significantly higher
47 levels of IFN-gamma were induced by DDA:TDB liposomes and liposome-uptake by
48 macrophages *in vitro* was also shown to be higher for DDA:TDB liposomes compared to
49 their cholesterol-containing counterparts, suggesting small changes in bilayer mechanics
50 can impact both on cellular interactions and immune responses.

51

52 **Keywords** Vaccine, Adjuvant, Cholesterol, Biodistribution, DDA, bilayer fluidity, liposomes,
53 subunit antigen.

54

55

56

57 **1. Introduction**

58 Liposomes composed of dimethyldioctadecylammonium (DDA) combined with an
59 immunostimulatory component of the mycobacterial cell wall, trehalose 6,6-dibehenate
60 (TDB) have been described as having immunostimulatory properties in numerous studies
61 [e.g. 1-5]. TDB is a synthetic analogue of trehalose 6,6 α -dimycolate (TDM) often referred to
62 as cord factor. Liposomes made of DDA and TDB, have been subject to stabilising and
63 sterilisation methods [6] with GMP production already successfully established [7]. An
64 intrinsic property of the DDA:TDB formulation is its ability to form a strong liposome-antigen
65 depot at the site of injection after administration via the subcutaneous (s.c.) or intramuscular
66 (i.m.) route [8], and this has been linked to the formulations ability to induce a powerful Th1
67 response as well as humoral immune responses [4, 5, 9]. In contrast, injection of antigen
68 alone, neutral liposomes, or PEGylated cationic liposomes all result in low levels of antigen
69 and adjuvant retention at the injection site and subsequently induce lower Th1 responses [8,
70 10, 11]. However, whilst all the formulations that promoted a depot effect were shown to
71 produce higher immune responses, direct targeting of liposomes to the lymphatics can
72 stimulate higher immune responses in some instances. One such study [12] investigated the
73 role of liposome-adjuvant delivery by comparing immune responses of mice immunised via
74 the intramuscular route and mice immunised via direct injection of the formulation into the
75 lymph node. Direct injection of DDA or DDA:TDB liposomes intralymphatically made no
76 notable difference to IgG1 responses in mice compared to those immunised intramuscularly.
77 However, IgG2a responses in mice were higher after intralymphatical administration of DDA
78 liposomes, but were not notably different when TDB was incorporated within the formulation
79 [12]. Similarly, the route of administration was shown to play a critical role in IFN-gamma
80 responses, with animals immunised with either DDA or DDA:TDB formulations directly into
81 the lymph node giving significantly higher responses compared to those immunised via the
82 intramuscular route. Based on these findings, it was important to consider various
83 formulation strategies that that facilitate the cationic lipid DDA to be used within the adjuvant
84 formulation, yet which would facilitate enhanced drainage to the lymphatics.

85

86 Cholesterol is an abundant component of mammalian cell membranes and has been
87 extensively studied in phospholipid liposomal systems as a membrane stabiliser [13 -15].
88 The incorporation of cholesterol into liposomal membranes has been shown to lead to
89 improved lipid packing consequently reducing or even eliminating the main phase transition
90 temperature [7,16,17]. The resulting lower gel to liquid phase transition temperature leads to
91 increased bilayer fluidity and liposomes show improved stability both *in vitro* and *in vivo* [13].
92 Whilst cholesterol is not inherently immunogenic, numerous studies have shown that

93 incorporation of cholesterol into liposomes leads to more favourable liposome properties
94 such as increased transfection rates [18] and improved immunogenicity [19].

95

96 Therefore within his present study, we have considered the impact of including cholesterol
97 within the DDA:TDB liposome adjuvant delivery system, with consideration of its ability to
98 modulate bilayer fluidity and potentially alter the pharmacokinetic profile of the liposomal-
99 adjuvant system. The packaging of cholesterol within the DDA:TDB bilayer was investigated
100 using surface pressure-area isotherms and differential scanning calorimetry. *In vitro* studies
101 investigating the ability of human macrophage-like cells to interact with liposomes containing
102 cholesterol at varying molar ratios were compared with *in vivo* performance, to investigate *in*
103 *vitro-in vivo* correlations. In addition, the ability of liposomes to form an antigen depot at the
104 site of injection, to present antigen to the immune system, and to generate an immune
105 response towards the co-administered antigen were investigated.

106

107 **2. Materials and Methods**

108 **2.1 Materials**

109 Dimethyldioctadecylammonium bromide (DDA) and trehalose 6,6'-dibehenate (TDB) were
110 purchased from Avanti Polar Lipids, Inc. (Alabaster, AL). Ag85B-ESAT-6 was kindly supplied
111 by Statens Serum Institute, Denmark. Cholesterol, hydrogen peroxide, Sephadex™ G-75
112 and bicinchoninic acid protein assay (BCA) components were purchased from Sigma Aldrich
113 (Dorset, UK). THP-1 cells were obtained from the American Type Culture Collection (via
114 LGC Standards, Middlesex, UK). Foetal calf serum (FCS) was from Biosera, UK. RPMI was
115 purchased from PAA (Yeovil, UK). Penicillin-streptomycin-glutamine (100X) was from
116 Invitrogen, Paisley, UK. For radiolabelling, 1-3-phosphatidyl[*N*-methyl-³H]choline, 1,2-
117 dipalmitoyl (³H-DPPC) was obtained from GE Healthcare (Amersham, UK), Pierce pre-
118 coated iodination tubes from Pierce Biotechnology (Rockford, IL) and ¹²⁵I (NaI in NaOH
119 solution), SOLVABLE™ and Ultima Gold™ scintillation fluid were purchased from Perkin
120 Elmer (Waltham, MA). Methanol and chloroform (both HPLC grade) were purchased from
121 Fisher Scientific (Leicestershire, UK). Tris-base, obtained from IDN Biomedical, Inc (Aurora,
122 Ohio) was used to make Tris buffer and adjusted to pH 7.4 using HCl; unless stated
123 otherwise Tris buffer was used at 10 mM, pH 7.4.

124

125 **2.2 Preparation and characterisation of liposomes**

126 Multilamellar vesicles (MLV) were prepared using the previously described lipid-film
127 hydration method [25]. Briefly, weighed amounts of DDA, TDB and cholesterol were
128 dissolved in chloroform/methanol (9:1, by volume) and the organic solvent was removed by

129 rotary evaporation followed by flushing with N₂ to form a thin lipid film which was hydrated in
130 10 mM Tris-buffer at pH 7.4 for 20 minutes at 60 °C, to a final concentration of 1.98 mM
131 DDA, 0.25 mM TDB and concentrations of cholesterol of 0, 18 or 31 mol% (8:1, 8:2:1 or
132 8:4:1 DDA:Chol:TDB molar ratio respectively). Ag85B-ESAT-6 antigen was added to
133 preformed vesicles to a final concentration of 10 µg/mL.

134

135 Physical characterisation of liposomes included vesicle size measurements (using dynamic
136 light scattering) and zeta potential analysis (using particle electrophoresis); both techniques
137 used a Brookhaven ZetaPlus (Brookhaven Instruments, Worcs, UK) to which 100 µL of
138 liposomes were resuspended in 3 ml Tris buffer (1 mM, pH 7.4).

139

140 **2.3 Langmuir-Blodgett Isotherms**

141 An automated controlled film balance apparatus (KSV Langmuir Mini-trough, KSV
142 Instruments Ltd., Helsinki, Finland) equipped with a platinum Wilhemy plate and placed on a
143 vibration-free table was used to collect the surface pressure-area isotherms as previously
144 reported [26]. The size of the trough was 24,225.0 mm² enclosing a total volume of
145 approximately 220 mL; the subphase was composed of filtered double-distilled water. Lipids
146 (at a fixed total concentration of 0.5 mg/mL⁻¹) were dissolved in chloroform and 20 µL of
147 each solution was spread onto the air/water interface with a Hamilton microsyringe,
148 (precision of ± 0.2 µL). After spreading, the monolayers were left for 10 minutes to allow the
149 chloroform to evaporate. Thereafter, the molecules underwent constant compression (10
150 mm/s⁻¹) until the required surface pressure of less than 0.2 mN/m was attained. The spread
151 monolayer was then compressed or expanded symmetrically with the two barriers until the
152 desired surface pressure was reached with accuracy within 0.1 mN/m. The experiment was
153 performed three times using monolayers prepared from different solutions, and with each
154 monolayer being compressed only once. KSV software (KSV Instruments Ltd) was used for
155 data analysis.

156

157 **2.4 Differential scanning calorimetry**

158 The gel-to-liquid phase transition temperatures were attained for the liposomal dispersions
159 via DSC and thermograms were acquired using a Pyris Diamond DSC (Perkin Elmer
160 Instruments LLC, USA). In this study, a scan rate of 10 °C/min was applied, over the range
161 of 25 °C to 80 °C. All scans were carried out in triplicate. Suspensions were contained in air
162 tight pans which were sealed immediately upon loading to reduce the effect of evaporation,
163 with a sample load weight of approximately 10 mg. A reference pan filled with an equal
164 volume of Tris buffer was used as a reference. This yielded an improved baseline,

165 achievable through a comparable thermal composition with the sample. Pyris software,
166 version 5.00.02 (Perkin Elmer Instruments LLC, USA) was used for all data analysis.

167

168 **2.5 Quantification of antigen loading and retention**

169 In order to measure antigen loading and to trace its distribution *in vivo*, Ag85B-ESAT-6
170 antigen was radio-labelled with ¹²⁵I using Pierce pre-coated iodination tubes containing
171 iodination reagent (Pierce Biotechnology, Rockford, IL) and a G-75 Sephadex
172 chromatography column for separation of ¹²⁵I-antigen from ¹²⁵I [8]. Antigen loading to the
173 various formulations was calculated by measuring radioactivity in supernatant and pellet
174 fractions after ultracentrifugation. To aid liposome sedimentation during centrifugation,
175 liposomes were placed in a solution of OVA (1 mg/mL) causing them to form a clear pellet,
176 and subsequently centrifuged twice (125,000 ×g, 4 °C, 1 hour) to ensure removal of all non-
177 associated antigen as previously reported [8]. Antigen release from liposomes stored in
178 simulated *in vivo* conditions was determined using liposomes adsorbing and entrapping
179 I125-labelled Ag85B-ESAT-6. Aliquots of each formulation were diluted (1:5) using 50 % v/v
180 FCS in Tris buffer and incubated in a shaking water bath at 37 °C for 96 h. At various time
181 intervals, samples were centrifuged and Ag85B-ESAT-6 release from liposomes was
182 calculated by recording the proportion of radioactivity recovered in the supernatant as a
183 percentage of the total radioactivity added.

184

185 **2.6 Immunisation procedures**

186 Five groups of five female C57BL/6 mice (6-10 weeks of age) received doses of liposome
187 vaccine formulations containing 2 µg of Ag85B-ESAT-6 in a 50 µL volume. One group also
188 received a non-liposome formulation containing 2 µg of Ag85B-ESAT-6 suspended in 50 µL
189 PBS. Naïve groups received 50 µL of PBS. Vaccine formulations were administered
190 intramuscularly, and each mouse received three doses at intervals of two weeks. Serum
191 samples were taken 12 days after the first injection and at two week intervals thereafter.

192

193 **2.6.1 Analysis of Ag85B-ESAT-6 specific antibody isotypes**

194 Serum samples were analysed for the presence of anti-Ag85B-ESAT-6 IgG, IgG1 and IgG2b
195 antibodies by enzyme-linked immunosorbent assay (ELISA). ELISA plates (flat bottom, high
196 binding) were coated with 50 µl Ag85B-ESAT-6 per well (3 µg/well) in PBS and incubated at
197 4 °C overnight. Plates were washed with phosphate buffered saline/tween buffer (PBST; 40
198 g NaCl, 1 g KCl, 1 g KH₂PO₄, 7.2 g Na₂HPO₄, (2H₂O) per 5 litres of ddH₂O, incorporating
199 ~0.4 ml of Tween 20) and blotted firmly onto paper towel. Plates were blocked with 100 µL
200 per well of 4 % w/v dried semi-skimmed milk powder in PBS. After 1 hour, plates were
201 washed again and serially-diluted serum samples added. Plates were incubated for 1 hour at

202 37 °C, followed by further washing and detection of anti-Ag85B-ESAT-6 antibodies using
203 horseradish peroxidase conjugated anti-mouse isotype specific immunoglobulins (goat anti-
204 mouse IgG1 and IgG2b), and subsequent addition of substrate solution, 2,2'-azino-bis (3-
205 ethylbenzthiazoline-6-sulfonic acid) (ABTS) in citrate buffer incorporating 5 µL of 30 %
206 H₂O₂/50 ml. After 20 minutes, the absorbance was measured at 405 nm using a plate reader
207 (Bio-Rad, Herts, UK).

208

209 **2.6.2 Proliferation of splenocytes *ex vivo***

210 To test cells for their ability to respond to antigen *in vitro*, splenocytes were restimulated with
211 various concentrations of antigen (0.05, 0.5, 5 µg/mL) and their proliferation, determined by
212 ³H-thymidine uptake, measured. On day 54 mice, (five groups of five mice, i.e. DDA:TDB,
213 DDA:Chol:TDB 8:2:1 and 8:4:1 molar ratio, antigen and naive) were terminated by cervical
214 dislocation and their spleens harvested and placed in a 7 mL bijoux containing 5 ml ice cold
215 PBS. Each spleen was treated individually and kept on ice until processing. Spleens were
216 gently grinded on a fine wire screen. After allowing the cell suspension to settle for
217 approximately 5 minutes the liquid was transferred to sterile 20 mL falcon tubes, without
218 disturbing the cellular debris at the bottom. The cell suspension was centrifuged at 1200
219 rpm, 15 °C for 10 minutes. After centrifugation the supernatant was removed, the cell
220 pellet re-suspended in 5 mL RPMI and a cell count performed. The cell number was
221 adjusted to between 8 x 10⁴ cells/ml.

222

223 For study of antigen specific proliferative responses, serial dilutions of Ag85B-ESAT-6
224 (0.05, 0.5 and 5 µg/ml) in RPMI were made and 100 µL added per well of a 96-well culture
225 plate. Wells containing medium only or 3 µg/mL of concanavalin A (ConA) were included in
226 all experiments as negative and positive controls respectively. Splenocytes (100 µL, 8 x 10⁴
227 cells/mL) were added to each well making a final well volume of 200 µl. Cultures were
228 incubated at 37 °C, 5 % CO₂, 95 % humidity for 72 h following which 18.5 kBq (0.5 µCi) ³H-
229 thymidine (40 µL in RPMI/well) was added. After a further 24 h incubation under the same
230 conditions, cells were harvested using a cell harvester (Titertek). For harvesting, media and
231 cells from each well was aspirated onto a quartz filter mat. Each mat was placed into a
232 plastic scintillation vial and 5 ml Ultima Gold™ scintillation fluid added/sample. All samples
233 were counted using a standard ³H scintillation counting protocol.

234

235 **2.6.3 Analysis of cytokine production**

236 Splenocytes isolated from mice were plated into 96-well plates (as described previously in
237 section 2.8.1). Cells were incubated for 40 hours at 37 °C, in a humid 5 % CO₂ environment,
238 after which supernatants were removed and stored at -70 °C for later analysis. Cytokine

239 levels of IL2, IL-5 and IFN- γ in the cell culture supernatants were quantified using the
240 DuoSet[®] capture ELISA kits), purchased from R&D systems, Abingdon, UK) according to the
241 manufacturer's instructions. Briefly, ELISA plates were first coated with capture antibody,
242 followed by washing and blocking. Samples of cell culture supernatants were then added
243 and cytokines quantified by addition of a biotinylated-detection antibody, detected by an
244 enzyme marker (Streptavidin-HRP) and substrate solution following repeated incubation and
245 washing steps. Absorbance was measured at 405 nm (Bio-Rad, Herts, UK).

246

247 **2.7 Biodistribution studies**

248 Inbred female BALB/c mice (6-10 weeks of age) were housed in cages within a laminar flow
249 safety enclosure and provided with irradiated food and filtered drinking water *ad libitum*. All
250 experiments adhered to the 1986 Scientific Procedures Act (UK) and were carried out in a
251 designated establishment. Four to six days prior to injection, two groups of mice were
252 injected subcutaneously with 200 μ L pontamine blue (0.5 % w/v in PBS). Pontamine blue is
253 an azo dye that has been described as being taken up by macrophages *in vivo* therefore
254 allowing for the identification of lymphoid tissue such as lymph nodes. Although pontamine
255 blue was primarily employed as a lymph node identification marker, it also served as a
256 marker for identification of infiltrating macrophages to the site of injection. Liposomes
257 containing the tracer molecule ³H-DPPC were produced as described previously [8]. To
258 obtain isotonicity, trehalose was added to the hydrating buffer to a final concentration of 10
259 % w/v. Mice were injected with Ag85B-ESAT-6 (radiolabelled with ¹²⁵I) adsorbing liposome
260 (radiolabelled with ³H) formulations (50 μ L/dose, i.m injection). At 1, 4 and 14 days post
261 injection (p.i) mice were terminated by cervical dislocation and tissue from the site of
262 injection (SOI), local draining lymph node (LN) and spleen removed for analysis of liposome
263 (³H) and antigen (¹²⁵I) presence using methods previously described elsewhere [8].

264

265 **2.8 Macrophage studies**

266 *In vitro* studies were performed using the human monocyte cell line THP-1 as previously
267 described [22, 23]. Briefly, THP-1 cells were resuspended in fresh medium (RPMI 1640 + 10
268 % v/v FCS) at a density of 5 x 10⁵ cells/mL and stimulated for 48 h with 250 nM
269 dihydroxyvitamin D3 (Enzo Life Sciences, Exeter UK) to differentiate cells. Prior to use, cells
270 were resuspended at 2 x 10⁶ cells/mL in fresh RPMI with 10 % v/v FCS. Liposomes (1
271 mg/mL) were labelled with 1,1'-dioctadecyl-3,3,3',3'-tetramethylindocarbocyanine
272 perchlorate) (DiIC) (0.1 mol%) by inclusion of the lipid (dissolved in solvent) in the solvent
273 evaporation stage of liposome production (as described in section 2.2). To ensure that all
274 formulations incorporated the DiIC fluorophore equally, the fluorescence was measured
275 using a fluorimeter. Fluorescently labelled liposomes were diluted to a concentration of 10

276 $\mu\text{g/mL}$ in RPMI, mixed with cells (1:1) in 6 well tissue culture plates and cocultured at $37\text{ }^\circ\text{C}$
277 in 5 % CO_2 . At various time-points, $500\text{ }\mu\text{L}$ of co-culture were removed and mixed with ice-
278 cold RPMI prior to immediate analysis. Association of fluorescent liposomes with THP-1
279 macrophages was analysed using non-fixed cells via flow cytometry using a Beckman-
280 Coulter FC500 cytometer (High Wycombe, UK). For each sample a minimum of 20,000
281 events were analysed.

282

283 **2.9 Statistical analyses**

284 Data was analysed using analysis of variance (ANOVA) followed by the Tukey test to
285 compare the mean values of different groups. Differences were considered significant when
286 the p value was less than 0.05.

287

288 **3. Results and discussion**

289 *3.1 The role of cholesterol in lipid packing.*

290 Cholesterol is a common component in liposomal formulations and its beneficial role as a
291 stabilising agent in liposomal bilayers is well recognised. Early studies investigating the
292 effect of liposome composition on drug retention [13] demonstrated that inclusion of 50 mol
293 % cholesterol within a liposome formulation increased the stability and reduced the
294 permeability of liposomal bilayers. At molar percentages between 20 - 50 % (depending on
295 the nature of the phospholipids), cholesterol can dissolve within the lipid bilayer, whereas at
296 higher concentrations cholesterol can form crystal habits [24].

297

298 To understand the effect of the incorporation of cholesterol on the spatial orientation of the
299 alkyl chains and the packing ability of DDA:TDB, initially we employed Langmuir studies [17]
300 and thermal analysis (Figure 1). Figure 1A shows the surface area and pressure isotherm
301 data of the various lipid combinations. The surface pressure/area isotherm of pure
302 cholesterol was typical for the structural characteristics of a sterol; up to a mean molecular
303 area of approximately $38\text{ }\text{\AA}^2/\text{molecule}$, the spread molecules show little interaction. After this
304 point, the molecules compact to form a condensed monolayer, with the molecules tightly
305 packed together (Figure 1A). Continued compression of this monolayer results in a collapse
306 of the monolayer at $45.4 \pm 0.4\text{ mN/m}$ and $32.5 \pm 1.1\text{ }\text{\AA}^2/\text{molecule}$. In contrast, DDA shows a
307 surface plot typical of a cationic lipid, where electrostatic repulsion between the head-groups
308 deters close proximity of the lipids. Hence the plot shows the transition of the monolayer as
309 compression is applied, initially starting as a gaseous monolayer, where the lipids are large
310 distance apart, through the expanded monolayer state to a condensed monolayer prior to
311 collapse (Figure 1A). In line with previous studies [21], the addition of TDB to DDA
312 liposomes aids packing of the monolayer, by presumably slotting between the cationic DDA

313 and reducing electrostatic repulsion. Upon addition of increasing amounts of cholesterol to
314 the DDA:TDB monolayer, the liquid-expanded phase transition seen with DDA:TDB was
315 removed and there was a direct transition from gaseous to liquid-condensed, with the overall
316 surface-pressure plot being more akin to the cholesterol plot at high cholesterol
317 concentrations (DDA:Chol:TDB 8:4:1 molar ratio; Figure 1A). This trend is supported by a
318 study on cholesterol inclusion within phosphatidylcholine (PC) systems, where Li et al [25]
319 report that ordered states can be formed faster with fewer packaging defects with
320 PC/cholesterol mixtures compared to PC alone [25]. Other studies [26] have also found that
321 cholesterol is able to generate a liquid-ordered phase in PC membranes containing more
322 than 25 mol % of cholesterol.

323 Differential scanning calorimetry (DSC) is a widely used method of thermal analysis that has
324 been applied to investigate and characterise a range of pharmaceutical systems [32]. DDA
325 lipid bilayers undergo a main phase transition at a characteristic temperature (T_c), with the
326 lipid chains transferring from a lower temperature gel-phase dominated by ordered alkyl
327 chain conformations, to a high-temperature fluid-phase characterised by disordered alkyl
328 chain conformations [28, 29]. From Figure 1B, the phase transition temperature of DDA:TDB
329 liposome (8:1 molar ratio) was $44.3 \pm 0.15^\circ\text{C}$. Upon addition of cholesterol (at an 8:2:1 molar
330 ratio; DDA:Chol:TDB molar ratio) there was a reduction in transition temperature to $42.7 \pm$
331 0.13°C (Figure 1B). The observation shows that cholesterol not only lowers the melting
332 temperature, but also the energy required, as the enthalpy required for the transition to occur
333 for DDA:TDB is 0.10 ± 0.01 J/g compared to the DDA:Chol:TDB (8:2:1 molar ratio) is $0.05 \pm$
334 0.01 J/g (Figure 1B). The hydrocarbon chains of lipids within DDA:TDB liposomes crystallise
335 into the rigid crystalline phase hence producing a T_c at $44.3 \pm 0.15^\circ\text{C}$. However, when
336 cholesterol is added at DDA:Chol:TDB 8:4:1 molar ratio, there is complete removal of the
337 transition temperature (Figure 1B) as the cholesterol prevents crystallisation of the
338 hydrocarbon chains. A similar study [17] has shown that the inclusion of cholesterol at 33 -
339 50 molar ratio % to liposomes formed of the lipid DSPC also removed the transition [17].

340 This removal of the gel-liquid crystalline phase transition of liposome vesicles may facilitate
341 enhanced fluidity of the system. Indeed, this was demonstrated by Coderch et al [30] who
342 showed that bilayer fluidity (and in their studies, skin penetration) was increased by the
343 addition of cholesterol to liposomes formulated from lipids with transition temperatures above
344 the environment they were being used in. Thus, in the case of DDA:TDB, which has a
345 transition temperature above body temperature, the addition of cholesterol to the liposomes
346 will increase their fluidity and therefore could impact on the biodistribution of the vesicles
347 after intramuscular injection.

348 *3.2 The effect of cholesterol on DDA:TDB liposome characteristics.*

349 From Figure 1 it was established that all three formulations tested gave high antigen loading;
350 due to their cationic nature these systems are able to electrostatically bind the anionic
351 antigen as previously reported [e.g. 7-11]. Inclusion of cholesterol into liposomes at a molar
352 ratio of 8:4:1 DDA:Chol:TDB was sufficient to remove the phase transition of the bilayer,
353 therefore a series of liposome formulations were prepared to consider the impact the
354 addition of cholesterol had on the liposome physico-chemical characteristics. From Table 1,
355 it can be seen that the incorporation of low levels of cholesterol to DDA:TDB liposomes
356 (8:2:1 molar ratio) did not make a significant difference to the vesicle size, but did reduce
357 antigen loading to a small extent (from 97% to 91%; Table 1). However, increasing
358 cholesterol content to a molar ratio of 8:4:1 DDA:Chol:TDB in the liposome formulation
359 resulted in a small increase in vesicle size and again a minor reduction in antigen loading
360 (Table 1). These small changes in size and antigen loading ability are most probably due to
361 the dilution of the overall cationic content of the liposomes as the cholesterol concentration is
362 increased. However, given these were only minor changes in the physico-chemical
363 characteristics, these would not be expected to have a notable impact on vaccine
364 performance, therefore using these formulations we then evaluated the impact of cholesterol
365 modified bilayer fluidity on liposomal adjuvant action, both with regards to the biodistribution
366 and the ability of the liposome to deliver and present antigen successfully.

367

368 *3.3 The impact of cholesterol induced fluidity on adjuvant function.*

369 Immunological analyses were undertaken to determine the efficacy of the three liposome
370 formulations (outlined in Table 1) in terms of antigen delivery and subsequent initiation of
371 detectable immune responses. Quantification of antigen specific IgG, IgG1, and IgG2b
372 antibody production, splenocyte proliferation and subsequent cytokine secretion were
373 analysed. Figure 2 shows the IgG (A), IgG1 and IgG2b (B) responses over time. As
374 expected, very little antibody production was noted when antigen was administered without
375 an adjuvant, whereas all liposome formulations were able to induce measurable levels
376 (Figure 2). When comparing between the formulations, only at day 12 were significant
377 differences noted with IgG responses from mice immunised with DDA:TDB being
378 significantly higher ($p < 0.05$) than DDA;Chol:TDB (8:4:1 molar ratio; Figure 2A). At all time-
379 points thereafter, there were no significant differences in antibody responses between the
380 formulations.

381 Splenocytes from immunised mice were cultured in the presence of Ag85B-ESAT-6 and their
382 proliferative abilities and cytokine production (cytokines IFN- γ , IL-2 and IL-5) measured.
383 Upon restimulation, mice which had been immunised with DDA:TDB liposomes adsorbing

384 Ag85B-ESAT-6 showed the highest levels of splenocyte proliferation, in line with previous
385 studies [13]. With increasing cholesterol content there was a trend, although not significant,
386 of reduced proliferation in response to secondary exposure to antigen (Fig. 3). In correlation
387 with previous reports [4,5] highlighting the strong Th1 mediating effects of DDA:TDB
388 liposomes, high levels of IFN- γ were noted when Ag85B-ESAT-6 was co-delivered with
389 DDA:TDB liposomes (Figure 4A). Whilst no significant differences between DDA:TDB and
390 DDA:Chol:TDB (8:2:1 molar ratio) liposomes was noted, inclusion of cholesterol at the higher
391 molar ratio of 8:4:1 resulted in significantly lower levels of IFN- γ and IL-2 ($p < 0.05$) compared
392 to non-cholesterol containing DDA:TDB liposomes (Fig 4A,B).

393 IFN- γ is an important correlate of protective immunity and numerous TB vaccine studies
394 have shown that IFN- γ production is important for TB vaccine efficacy [6, 31, 32]. IL-2 is
395 another essential signal in directing cell mediated immunity [38], whilst also playing a role in
396 the humoral response. The production of IL-5 was also investigated as a signal of Th2
397 polarising abilities; in line with previous studies investing DDA:TDB liposomes, significantly
398 higher levels of IL-5 were produced compared to delivery of free antigen; however, no
399 differences were noted between liposomal groups (results not shown). Recent studies [34]
400 investigating the effect of membrane fluidity compared the immune responses of DDA:TDB
401 liposomes with liposomes composed of its unsaturated analog dimethyldioleoylammonium
402 (DODA), the latter of which forms fluid disordered phase liposomes. These studies found
403 that DDA-based liposomes induced a significantly higher immune response compared to that
404 obtained with the fluid DODA-based liposomes. This is comparable to the finding in this
405 study; as the cholesterol content within the liposome formulation is increased, the fluidity of
406 the bilayer decreases and a reduction in Th1-biased responses are reduced.

407

408 *3.4 The impact of cholesterol incorporation within DDA:TDB liposomes on their clearance* 409 *from the injection site.*

410 The role of cholesterol in eliciting a liposome or antigen depot-effect at the site of injection,
411 and the subsequent presence of either component in the local lymph nodes, was
412 investigated. As cholesterol inclusion at a 8:2:1 molar ratio had no effect in the
413 aforementioned immunisation studies, only the higher proportion of cholesterol (8:4:1 molar
414 ratio) was compared against the non-cholesterol containing counterpart. Figure 5 shows the
415 presence of liposome and Ag85B-ESAT-6 antigen at the SOI after i.m. injection of antigen
416 adsorbing formulations. DDA:TDB and DDA:Chol:TDB liposomes (Figure 5A) and their
417 associated antigen (Figure 5B) showed no significant difference in clearance rates from the
418 injection site, with between 40 - 50 % of the original liposome dose being recovered 2 weeks
419 p.i. (Figure 5A). With regards to movement of vaccine components to the local draining

420 lymph node, the data suggests the DDA:TDB liposomes accumulate more rapidly at the
421 draining lymph nodes over the first 4 days, with accumulation normalising by day 14
422 between the groups (Figure 5C), yet drainage of the antigen was not influenced by the
423 presence of cholesterol in the bilayer formulation (Figure 5D). When considering the
424 movement of infiltrating monocytes to the site of injection [8, 11], there was no notable
425 difference in the intensity of monocyte recruitment to the injection site when cholesterol was
426 included into DDA:TDB liposomes (Figure 5E).

427

428 From Figure 5 it can be seen that whilst initially high-levels of both liposomes and antigen
429 are retained at the site of injection (~80 %; Figure 5 A and B). However by day 4, liposome
430 levels remain at similar levels, yet antigen levels drop to ~20 % (Figure A and B), suggesting
431 that the liposomes may not be able to retain high levels of antigen over a longer period. To
432 consider the ability of these liposome systems to retain antigen, an antigen retention study
433 was conducted in simulated *in vivo* conditions (Figure 5F). These results show that whilst the
434 liposomes +/- cholesterol have similar zeta potential and antigen loading in the suspension
435 buffer prior to injection; however, when in the presence of other proteins (such as might be
436 found at the injection site, promoting liposome aggregation depot formation), competition for
437 electrostatic binding to the cationic liposomes may occur resulting in antigen loss. Further,
438 the ability of liposomes to retain antigen may also be influenced by cholesterol content
439 (Figure 5E).

440

441 In a previous study where the movement of vaccine components from the SOI was studied,
442 more rapid draining of the liposome component was observed when DDA was substituted for
443 its unsaturated counterpart 'DODA' (which results in more fluid liposomes) [34]. However,
444 whilst here we see that cholesterol inclusion alters the fluidity of DDA:TDB liposomes (when
445 included at a 8:4:1 molar ratio), this does not translate into altered draining from the injection
446 site, nor to the draining lymph node after 14 days. However with both formulations, antigen
447 loss from the depot at the injection site was noted. The reduction in vaccine efficacy seen in
448 DDA:Chol:TDB (8:4:1 molar ratio) liposomes must therefore be due to a separate factor;
449 looking at other studies [34, 35] which have analysed the presence of adjuvant and antigen
450 in APCs, an important correlation between co-localization of both components and
451 successful responses was seen. Indeed recent studies by Kamath et al. [35] have shown
452 that synchronisation of dendritic cell activation and antigen exposure is required for the
453 induction of Th1 responses, but only a small population of DCs require such activation to
454 promote strong Th1 responses [35]. In these studies the authors demonstrated that mice
455 immunised with antigen and DDA/TDB liposomes separately but to the same injection site,
456 induced similar Th2 responses, but weaker Th1 responses than mice immunised with

457 DDA/TDB with adsorbed antigen [34]. Similarly in another study [36], antigen administered
458 alone, one day prior to a standard vaccine was shown to be detrimental for the immune
459 response, due to the early exposure of APCs to free antigen. Overall, these studies [35, 36]
460 demonstrate that whilst the depot-effect is important, more important and detrimental to the
461 ensuing immune response is the pre-exposure of dendritic cells to antigen alone which can
462 mediate temporary anergy. Therefore inclusion of cholesterol within the formulation may
463 result in more rapid loss of antigen initially which subsequently normalises between the
464 formulations, but which could result in increased pre-exposure of DC to antigen alone,
465 reducing Th1 responses.

466

467 *3.5 Interaction of cholesterol containing DDA:TDB liposomes with phagocytes*

468 Given that the difference in bilayer packaging and transition temperature of the DDA:TDB
469 liposomes formulated with or without cholesterol had no impact on biodistribution but did
470 impact on Th1 responses, this would suggest that cellular uptake and activation may be
471 playing a key role in promoting the different immune responses noted. Therefore to quantify
472 liposome uptake by phagocytes, the human continuous cell line THP-1 was used.
473 Fluorescence-labelled DDA:TDB and DDA:Chol:TDB (8:2:1 and 8:4:1 molar ratio) liposomes
474 were co-cultured with THP-1-derived macrophages at a final lipid concentration of 5 µg/mL.
475 The proportion of macrophages associated with fluorescent liposomes, and the relative
476 amount of fluorescence associated, was quantified using flow cytometry. Figure 6 shows the
477 time-dependent uptake of DDA:TDB liposomes (\pm cholesterol) after application to THP-
478 derived macrophages at 37°C; with increased amounts of cholesterol, each cell associates
479 with fewer liposomes, as evidenced by less fluorescence (Figure 6B). For DDA:TDB
480 liposomes, around 75 % of the cells were associated with the liposomes (Figure 6C), which
481 is in line with previous studies [23]. However, with increasing cholesterol content the
482 percentage of cells associated with liposomes decreased to ~ 40 % (Figure 6C). Although
483 the data presented suggests uptake of DDA:TDB liposomes by macrophage in vitro was
484 higher compared to cholesterol-containing counterparts it is possible that the activity of
485 DDA:TDB liposomes in the presence/absence of cholesterol may be different in vivo,
486 particularly given the in vivo biodistribution suggests the liposomes and antigen are present
487 at the injection site for several days.

488 From these studies it can be seen that the cholesterol content within the liposomes reduces
489 liposomal uptake by phagocytes and this may be the contributing factor in the reduced Th1
490 responses noted in Figure 3 and 4. As found in a number of studies [8, 11], upon injection
491 with a vaccine antigen, DDA-based liposomes form a vaccine depot at the injection site that
492 results in a continuous attraction of antigen-presenting cells that engulf a high amount of

493 adjuvant. These cells are subsequently efficiently activated, as measured by an elevated
494 expression of the co-stimulatory molecules CD40 and CD86 [34]. Furthermore, a study by
495 Korsholm et al (2007) [36] proposed that cationic DDA liposomes promote uptake via
496 endocytosis prior to disruption or fusion with internal cellular membranes, and that the
497 delivery of associated antigen to cells occurs upon instant contact with the cell surface
498 through electrostatic interactions prior to active antigen uptake and presentation, which is a
499 key mechanism behind the adjuvant properties of cationic DDA liposomes. In addition,
500 inclusion of DSPC into DDA demonstrated that antigen acquisition by APCs was dependent
501 upon DDA concentration [36].

502

503 **4. Conclusion**

504 In this study, the aim was to investigate the role of cholesterol in the DDA:TDB adjuvant
505 delivery system. Inclusion of ~30 mol% of cholesterol was able to abolish the transition
506 temperature of the liposome formulation without notable impact of the vesicle size, zeta
507 potential and antigen loading. However, whilst inclusion of cholesterol within the DDA:TDB
508 liposomal adjuvant system could enhance the fluidity of the system, this did not translate to
509 increased movement to the local lymphatics, nor impact on the recruitment of monocytes to
510 the injection site, yet it resulted in a reduction in Th1-based immune responses. This would
511 suggest that the reduction in immune responses is most likely a result of reduced APC
512 uptake.

513

514 The effect of membrane fluidity has been investigated previously with the use of cationic lipid
515 DODA exhibiting a low phase transition temperature. In accordance with the results
516 presented here, these 'fluid' liposomes also showed a decreased ability to stimulate
517 splenocytes to produce the Th1 biased cytokine IFN- γ . It is possible that the increased
518 liposome rigidity noted with DDA:TDB liposomes, as compared to those including
519 cholesterol, results in increased exposure of immune cells to the co-presented antigen.
520 Supporting this theory, the flow cytometry results presented show a clear increase in
521 liposome uptake of non-cholesterol containing DDA:TDB liposomes.

522

523 The results presented in this study show that a balance between physico-chemical
524 properties and desired immunological outcome must be considered. Although cholesterol is
525 widely considered a suitable liposome stabilising compound, we have shown that the strong
526 Th1 cytokine polarising nature of TDB containing DDA liposomes is forfeited by addition of
527 cholesterol to levels of ~30 mol% to this liposome formulation.

528 **Acknowledgements**

529 This work was partly funded by NewTBVAC (contract no.HEALTHF3-2009-241745).
530 NewTBVAC has been made possible by contributions from the European Commission.

531

532 **Supporting Information Available**

533 This information is available free of charge via the Internet at <http://pubs.acs.org/>.

534

535 **References**

536 1. Andersen, P. Effective vaccination of mice against Mycobacterium tuberculosis infection
537 with a soluble mixture of secreted mycobacterial proteins. *Infect. Immun.* **1994**, *62*, 2536-
538 2544.

539 2. Lindblad, E.; Elhay, M.; Silva, R.; Appelberg, R.; Andersen, P. Adjuvant modulation of
540 immune responses to tuberculosis subunit vaccines. *Infect. Immun.* **1997**, *65*, 623-629.

541 3. McNeil, S.; Rosenkrands, I.; Agger, E.-M.; Andersen, P.; Perrie, Y. Subunit vaccines:
542 distearoylphosphatidylcholine-based liposomes entrapping antigen offer a neutral alternative
543 to dimethyldioctadecylammonium-based cationic liposomes as an adjuvant delivery system.
544 *J. Pharm. Sci.* **2011**, *100*, 1856-1865.

545 4. Kirby, D.; Kaur, R.; Agger, E.-M.; Bramwell, V.; Andersen, P.; Perrie, Y. Developing solid
546 particulate vaccine adjuvants - surface bound antigen favouring a humoural response,
547 whereas entrapped antigen shows a tendency for cell mediated immunity. *Curr. Drug. Deliv.*
548 **2013**, *10*, 268-278.

549 5. Lemaire, G.; Tenu, J.; Petit, J.; Lederer, E. Natural and synthetic trehalose diesters as
550 immunomodulators. *Med. Res. Rev.* **1986**, *6*, 243-274.

551 6. Mohammed, A.; Bramwell, V.; Kirby, D.; McNeil, S.; Perrie, Y. Increased Potential of a
552 Cationic Liposome Based Delivery System: Enhancing Stability and Sustained
553 Immunological Activity in Pre-Clinical Development *Eur. J. Pharm. Biopharm.* **2010**, *76*, 404-
554 412.

555 7. Christensen, D.; Agger, E.-M.; Andreasen, L.; Kirby, D.; Andersen, P.; Perrie, Y.
556 Liposome-based cationic adjuvant formulations (CAF): Past, present, and future. *J.*
557 *Liposome Res.* **2009**, *19*, 2-11.

558 8. Henriksen-Lacey, M.; Bramwell, V.; Christensen, D.; Agger, E.-M.; Andersen, P.; Perrie,
559 Y. Liposomes based on dimethyldioctadecylammonium promote a depot effect and enhance
560 immunogenicity of soluble antigen. *J. Control. Release* **2010**, *142*, 180-186.

561 9. Vangala, A.; Bramwell, V.; McNeil, S.; Christensen, D.; Agger, E.-M.; Perrie, Y.
562 Comparison of vesicle based antigen delivery systems for delivery of hepatitis B surface
563 antigen. *J. Control. Release* **2007**, *119*, 102-110.

564 10. Kaur, R.; Bramwell, V.; Kirby, D.; Perrie, Y. Pegylation of DDA:TDB liposomal adjuvants
565 reduces the vaccine depot effect and alters the Th1/Th2 immune responses. *J. Control.*

566 *Release* **2012**, *158*, 72-77.

567 11. Kaur, R.; Bramwell, V.; Kirby, D.; Perrie, Y. Manipulation of the surface pegylation in
568 combination with reduced vesicle size of cationic liposomal adjuvants modifies their
569 clearance kinetics from the injection site, and the rate and type of T cell response. *J. Control.*
570 *Release* **2012**, *168*, 331-337.

571 12. Mohanan, D.; Slutter, B.; Henriksen-Lacey, M.; Jiskoot, W.; Bouwstra, J.; Perrie, Y.;
572 Kundig, T.; Gander, B.; Johansen, P. Administration routes affect the quality of immune
573 responses: a cross-sectional evaluation of particulate antigen-delivery systems. *J. Control.*
574 *Release* **2010**, *147*, 342-349.

575 13. Gregoriadis, G.; Davis, C. Stability of liposomes in vivo and in vitro is promoted by their
576 cholesterol content and the presence of blood cells. *Biochem. Bioph. Res. Comm.* **1979**, *89*,
577 1287-1293.

578 14. McMullen, T.; McElhaney, R. Physical studies of cholesterol-phospholipid interactions.
579 *Curr Opin. Colloid Interface Sci.* **1996**, *1*, 83-90.

580 15. Sulkowski, W.; Pentak, D.; Nowak, K.; Sulkowska, A. The influence of temperature,
581 cholesterol content and pH on liposome stability. *J. Mol. Struct.* **2005**, *744-747*, 737-747.

582 16. Ohtake, S.; Schebor, C.; Palecek, S.; Pablo, J. Phase behavior of freeze-dried
583 phospholipid-cholesterol mixtures stabilized with trehalose. *Biochim. Biophys. Acta* **2005**,
584 *1713*, 57-64.

585 17. Moghaddam, B.; Ali, H.; Wilkhu, J.; Kirby, D.; Mohammed, A.; Zheng, Q.; Perrie, Y. The
586 application of monolayer studies in the understanding of liposomal formulations. *Int. J.*
587 *Pharm.* **2011**, *417*, 235-244.

588 18. Xu, L.; Anchordoquy, T. Cholesterol domains in cationic lipid/DNA complexes improve
589 transfection. *Biochim. Biophys. Acta* **2008**, *1778*, 2177-2181.

590 19. Bakouche, O.; Gerlier, D. Enhancement of immunogenicity of tumour virus antigen by
591 liposomes: the effect of lipid composition. *Immunology* **1986**, *58*, 507-513.

592 20. Bangham, A.; Standish, M.; Watkins, J. Diffusion of univalent ions across the lamellae of
593 swollen phospholipids. *J. Mol. Biol.* **1965**, *13*, 238-252.

594 21. Christensen, D.; Kirby, D.; Foged, C.; Agger, E.-M.; Andersen, P.; Perrie, Y.; Nielsen, H.
595 alpha,alpha'-trehalose 6,6'-dibehenate in non-phospholipid-based liposomes enables direct
596 interaction with trehalose, offering stability during freeze-drying. *Biochim. Biophys. Acta*
597 **2008**, *1778*, 1365-1373.

598 22. Torr, E.; Gardner, D.; Thomas, L.; Goodall, D.; Bielemeier, A.; Willetts, R.; Griffiths, H.;
599 Marshall, L.; Devitt, A. Apoptotic cell-derived ICAM-3 promotes both macrophage
600 chemoattraction to and tethering of apoptotic cells. *Cell. Death Differ.* **2012**, *19*, 671-679.

601 23. Henriksen-Lacey, M.; Devitt, A.; Perrie, Y. The vesicle size of DDA:TDB liposomal
602 adjuvants plays a role in the cell-mediated immune response but has no significant effect on

603 antibody production. *J. Control. Release* **2011**, *154*, 131-137.

604 24. Egelhaaf, R.; Epend, R.; Maekawa, S. The arrangement of cholesterol in membranes
605 and binding of NAP-22. *Chem. Phys. Lipids* **2003**, *122*, 33-39.

606 25. Li, X.-M.; Momsen, M.; Smaby, J.; Brockman, H.; Brown, R. Cholesterol Decreases the
607 Interfacial Elasticity and Detergent Solubility of Sphingomyelins. *Biochemistry* **2001**, *40*,
608 5954-5953.

609 26. Thewalt, J.; Bloom, M. Phosphatidylcholine: cholesterol phase diagram *Biophys J* **1991**,
610 *63*, 1178-1181.

611 27. Giron, D. Applications of thermal analysis and coupled techniques in the pharmaceutical
612 industry. *J. Thermal Anal.* **2002**, *68*, 335-357.

613 28. Bloom, M.; Evans, E.; Mouritsen, O. Physical-properties of the fluid lipid-bilayer
614 component of cell membranes - a perspective. *Q. Rev. Biophys.* **1991**, *24*, 293-397.

615 29. Vangala, A.; Kirby, D.; Rosenkrands, I.; Agger, E.-M.; Andersen, P.; Perrie, Y. A
616 comparative study of cationic liposome and niosome-based adjuvant systems for protein
617 subunit vaccines: characterisation, environmental scanning electron microscopy and
618 immunisation studies in mice. *J. Pharm. Pharmacol.* **2006**, *58*, 787-799.

619 30. Coderch, L.; Fonollosa, J.; De Pera, M.; Estelrich, J.; De La Maza, A.; Parra, J. Influence
620 of cholesterol on liposome fluidity by EPR. Relationship with percutaneous absorption. *J.*
621 *Control. Release* **2000**, *68*, 85-95.

622 31. Agger, E.-M.; Andersen, P. Tuberculosis subunit vaccine development: on the role of
623 interferon-gamma. *Vaccine* **2001**, *19*, 2298-2302.

624 32. Agger, E.-M.; Rosenkrands, I.; Hansen, J.; Brahimi, K.; Vandahl, B.; Aagaard, C.;
625 Werninghaus, K.; Kirschning, C.; Lang, R.; Christensen, D.; Theisen, M.; Follmann, F.;
626 Andersen, P. Cationic liposomes formulated with synthetic mycobacterial cordfactor
627 (CAF01): a versatile adjuvant for vaccines with different immunological requirements. *PLoS*
628 *ONE* **2008**, *3*, 3116.

629 33. Playfair, J.; Bancroft, G., *Infection and Immunity*. Oxford University Press: Oxford, 2004.

630 34. Christensen, D.; Henriksen-Lacey, M.; Kamath, A.; Linderstrom, T.; Korsholm, K.;
631 Christensen, J.; Rochat, A.; Lambert, P.-H.; Andersen, P.; Siegrist, C.-A.; Perrie, Y.; Agger,
632 E.-M. A cationic vaccine adjuvant based on a saturated quaternary ammonium lipid have
633 different in vivo distribution kinetics and display a distinct CD4 T cell-inducing capacity
634 compared to its unsaturated analog. *J. Control. Release* **2012**, *160*, 468-476.

635 35. Kamath, A.; Mastelic, B.; Christensen, D.; Rochat, A.-F.; Agger, E.-M.; Pinschewer, D.;
636 Andersen, P.; Lambert, P.-H.; Siegrist, C.-A. Synchronization of dendritic cell activation and
637 antigen exposure is required for the induction of Th1/Th17 responses. *J. Immunol* **2012**,
638 *188*, 4828-4837.

639 36. Korsholm, K.; Agger, E.-M.; Foged, C.; Christensen, D.; Dietrich, J.; Andersen, C.-S.;

640 Geisler, C.; Andersen, P. The adjuvant mechanism of cationic
641 dimethyldioctadecylammonium liposomes. *Immunology* **2007**, *121*, 216-226.

642

643

644

645

646

647

648

649

650

651

652

653

654

655

656

657

658

659

660

661

662

663

664

665

666

667

668 **Tables and Figures**

669
670 **Table 1. Characteristics of cationic liposomes.**
671

| Formulation | Molar ratio | Size ± SD (nm) | Zeta-potential ± SD (mV) | Antigen loading (%) |
|--------------|-------------|----------------|--------------------------|---------------------|
| DDA:TDB | 8:1 | 586 ± 78 | 52 ± 5 | 97 ± 2.1 |
| DDA:Chol:TDB | 8:2:1 | 663 ± 66 | 47 ± 6 | 91 ± 1.1* |
| DDA:Chol:TDB | 8:4:1 | 737 ± 53* | 45 ± 3 | 87 ± 3.6* |

672 Vesicle size, zeta-potential and antigen loading of DDA:TDB formulations with and without
673 the addition of cholesterol. Size and zeta-potential were measured in Tris buffer (1 mM)
674 using a Brookhaven ZetaPlus instrument. Antigen loading was measured using radiolabelled
675 antigen. Results represent mean ± SD of triplicate experiments. *denotes $p < 0.01$ or greater
676 in comparison to DDA:TDB.
677

678 Figure 1. The effect of cholesterol on lipid packing. A) Compression isotherm studies of the
679 pure and mixture of lipid monolayers of DDA, cholesterol, DDA:TDB with the addition of
680 cholesterol at two different molar ratios 2 and 4 in deionised water at 20 °C. Results are
681 expressed as the means of three experiments. SD has not been shown for clarity. B) DSC
682 thermograms of the gel-to-liquid phase transition of DDA:TDB formulations with the addition
683 of cholesterol at two different molar ratios 2 and 4. Liposomes were produced via lipid
684 hydration in 10 mM Tris buffer (pH 7.4). DSC Thermograms were made at 10 °C/minute (600
685 °C/h) over the tested temperature range of 25-80 °C One of three thermograms for each
686 vesicle system is shown with the results representative of three independent experiments.

687 Figure 2. Ag85B-ESAT-6 specific antibody titres. Groups of five female C57Bl/6,
688 approximately six weeks old, received doses of liposome formulations containing 2 µg of
689 Ag85B-ESAT-6 in a 50 µL volume. Vaccine formulations were administered intramuscularly,
690 and each mouse received three doses at intervals of two weeks. Serum samples were taken
691 at 12 days after the first administration and at two week intervals thereafter. Anti-Ag85B-
692 ESAT-6 IgG responses (A) the IgG1/IgG2a balance over the period of the study (B) are
693 shown; anti-Ag85B-ESAT-6 IgG1 and IgG2b were measured by enzyme-linked
694 immunosorbent assay (ELISA). Results represent mean ± SD reciprocal end point serum
695 dilution (\log_{10}) from five mice. ***Denotes significantly increased antibody titres ($p < 0.05$)
696

697 Figure 3. Spleen cell proliferation in response to Ag85B-ESAT-6 antigen. Cell proliferation
698 was measured by incorporation of ³H-thymidine into cultured splenocytes derived from mice
699 immunised with Ag85B-ESAT-6 antigen containing formulations. Results represent mean ±
700 SD of five mice.
701

702 Figure 4. Ag85B-ESAT-6 specific cytokine production. Cytokines were detected using
703 DuoSet® capture ELISA kits (mouse IFN- γ (A), IL-2 (B), purchased from R&D systems,
704 Abingdon, UK) according to the manufacturer's instructions. Results shown mean \pm SD,
705 n=5. * denotes significantly increased levels in comparison to naïve controls (n=5, p<0.05).

706

707 Figure 5. Presence of liposome and antigen at the site of injection following intramuscular
708 injection of Ag85B-ESAT-6 antigen adsorbing to DDA:TDB with and without cholesterol.
709 Tissue was collected on days 1, 4 and 14 p.i and assayed for the presence of ^3H and ^{125}I
710 relating to A) liposome and B) antigen at the site of injection, C) liposome and D) antigen at
711 the popliteal lymph node respectively. Results represent mean \pm SD of four mice. E) shows
712 monocyte infiltration (tracked by pontamine blue) at the SOI (quadriceps) after 14 days
713 injection (i.m.) of DDA:TDB and DDA:Chol:TDB (8:4:1 molar ratio) liposomes with adsorbed
714 Ag85B-ESAT-6 antigen. F) Ag85B-ESAT-6 antigen release profile of DDA:TDB, 8:2:1 and
715 8:4:1 liposomes using ^{125}I -labelled Ag85B-ESAT-6 when stored under simulated *in vivo*
716 conditions (50 % FCS, 37 °C). Results represent mean \pm SD of triplicate experiments.

717

718 Figure 6. The presence of cholesterol in liposomes reduces their interaction with THP-1
719 cells. THP-1-derived macrophages were co-cultured with dilC-fluorescently labeled
720 liposomes with the addition of cholesterol at two different molar ratios 2 and 4. At the
721 indicated timepoints, a sample of cells was removed and immediately analysed using flow
722 cytometry. Data from a minimum of 20,000 cells are shown: (A) frequency histograms for
723 fluorescence associated (surface-bound or internalised) with macrophages at the indicated
724 times, from a representative assay. (B) Mean fluorescence intensity of macrophages
725 cocultured with the indicated liposomes. (C) Percentage of macrophages positive for
726 fluorescence. Data shown for parts (B) and (C) are mean \pm SEM from three independent
727 experiments. Statistical analyses used ANOVA with Dunnett's post test. *P<0.05 compared
728 to DDA:TDB (8:1 molar ratio) at each time point.

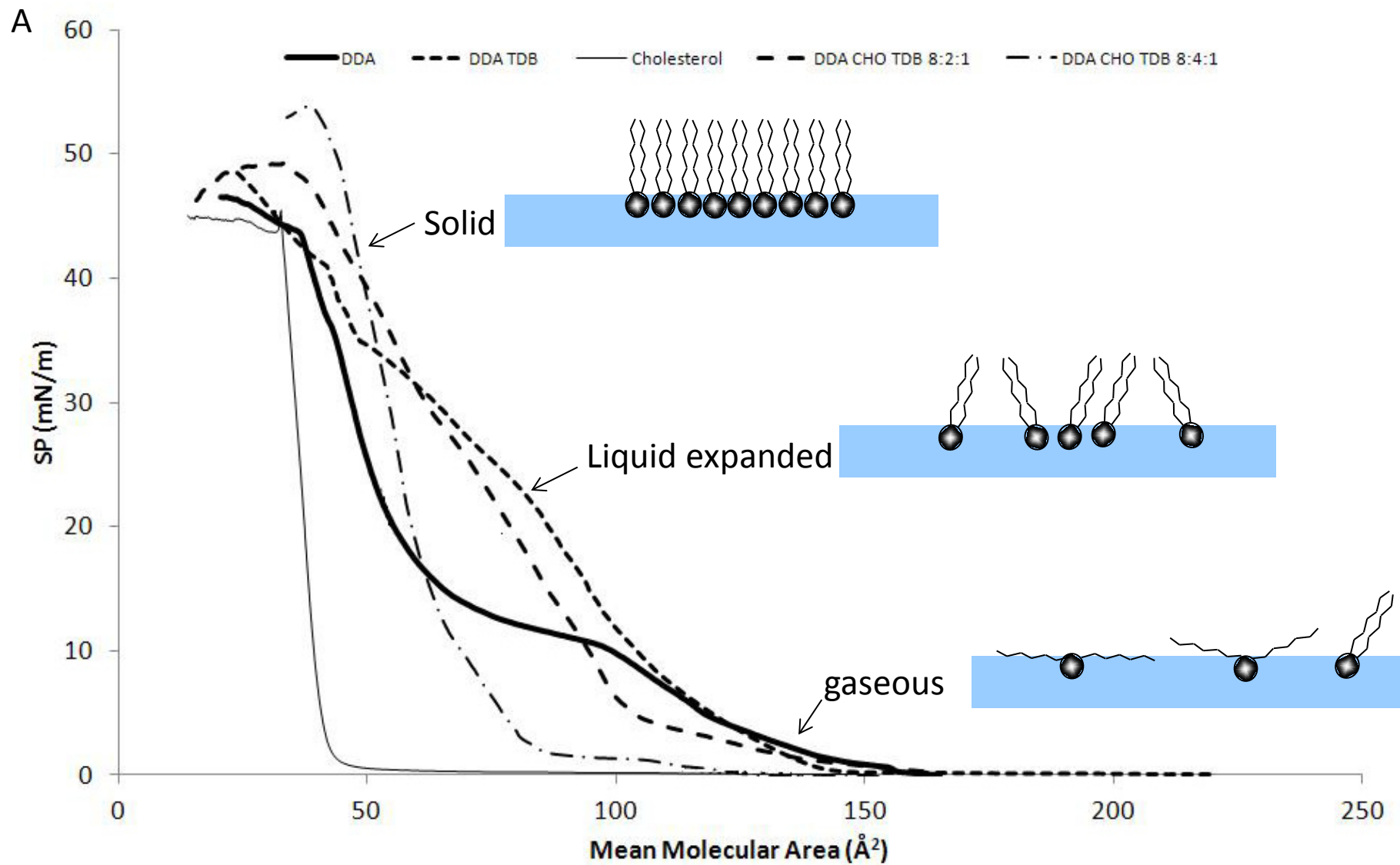


Figure 1A

B

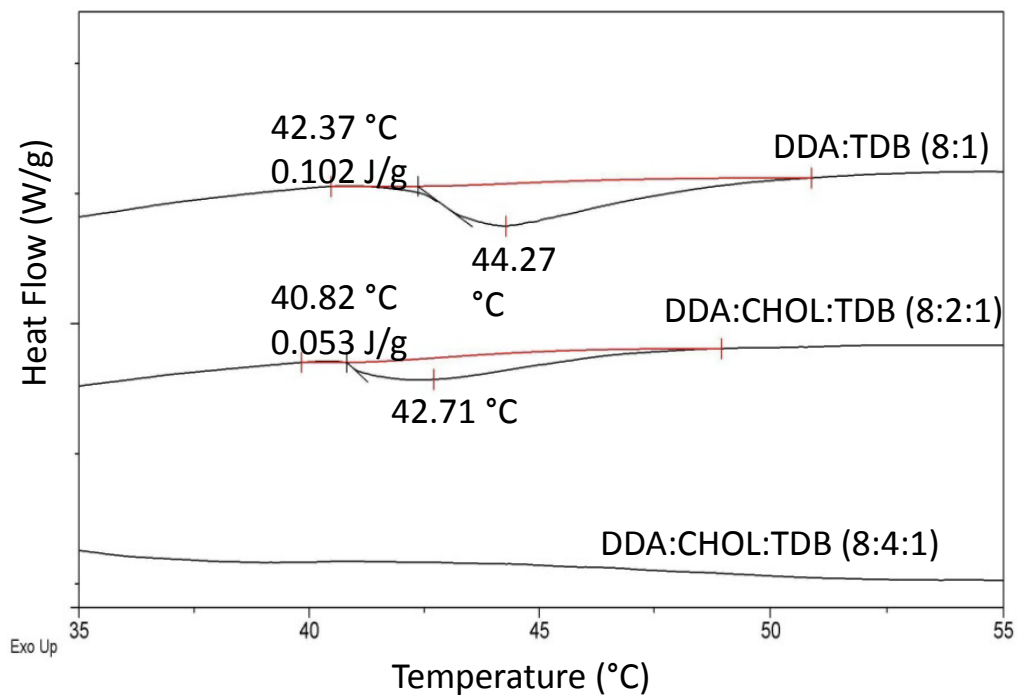
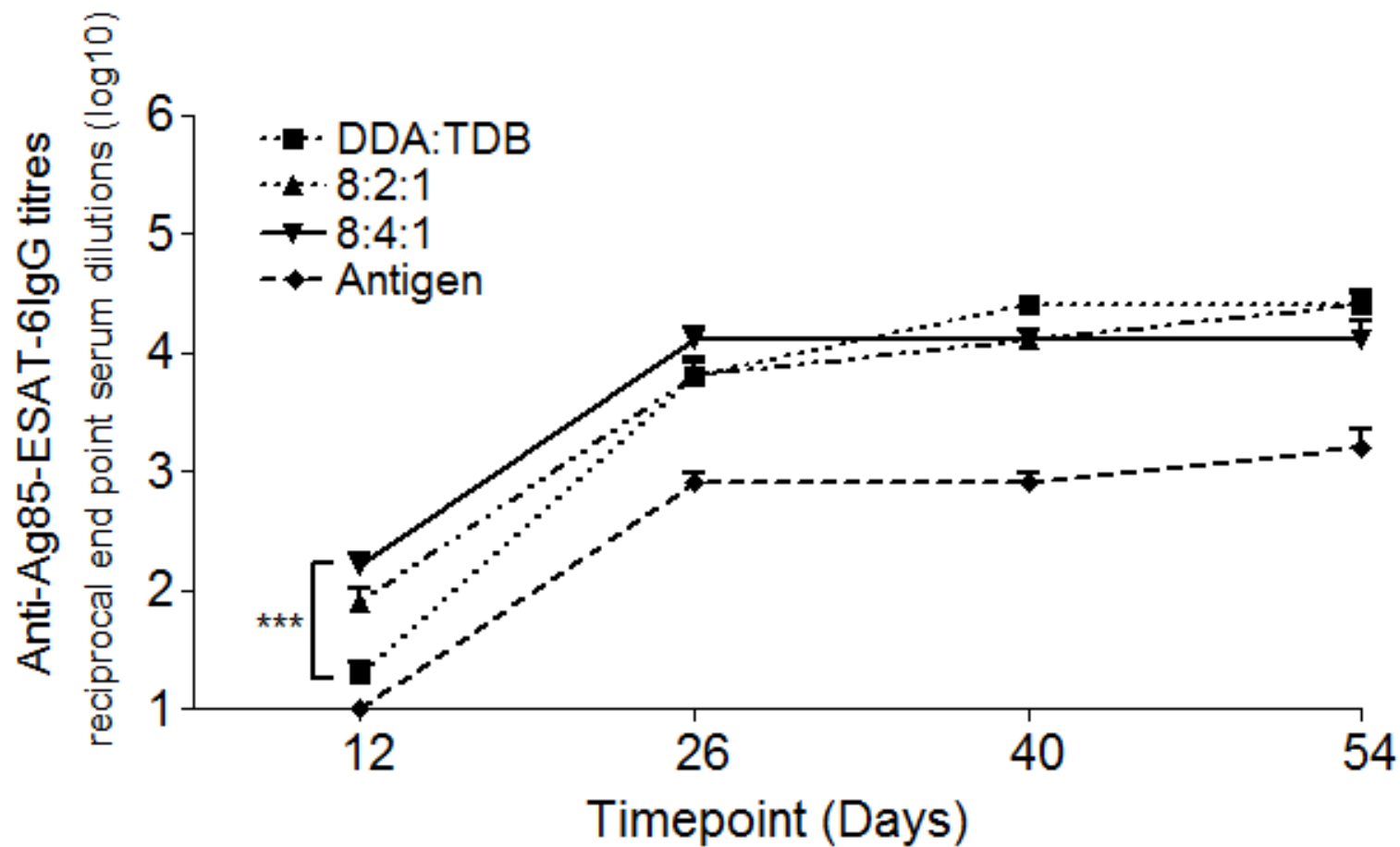


Figure 1B

A



Reciprocal end point serum dilution (\log_{10})

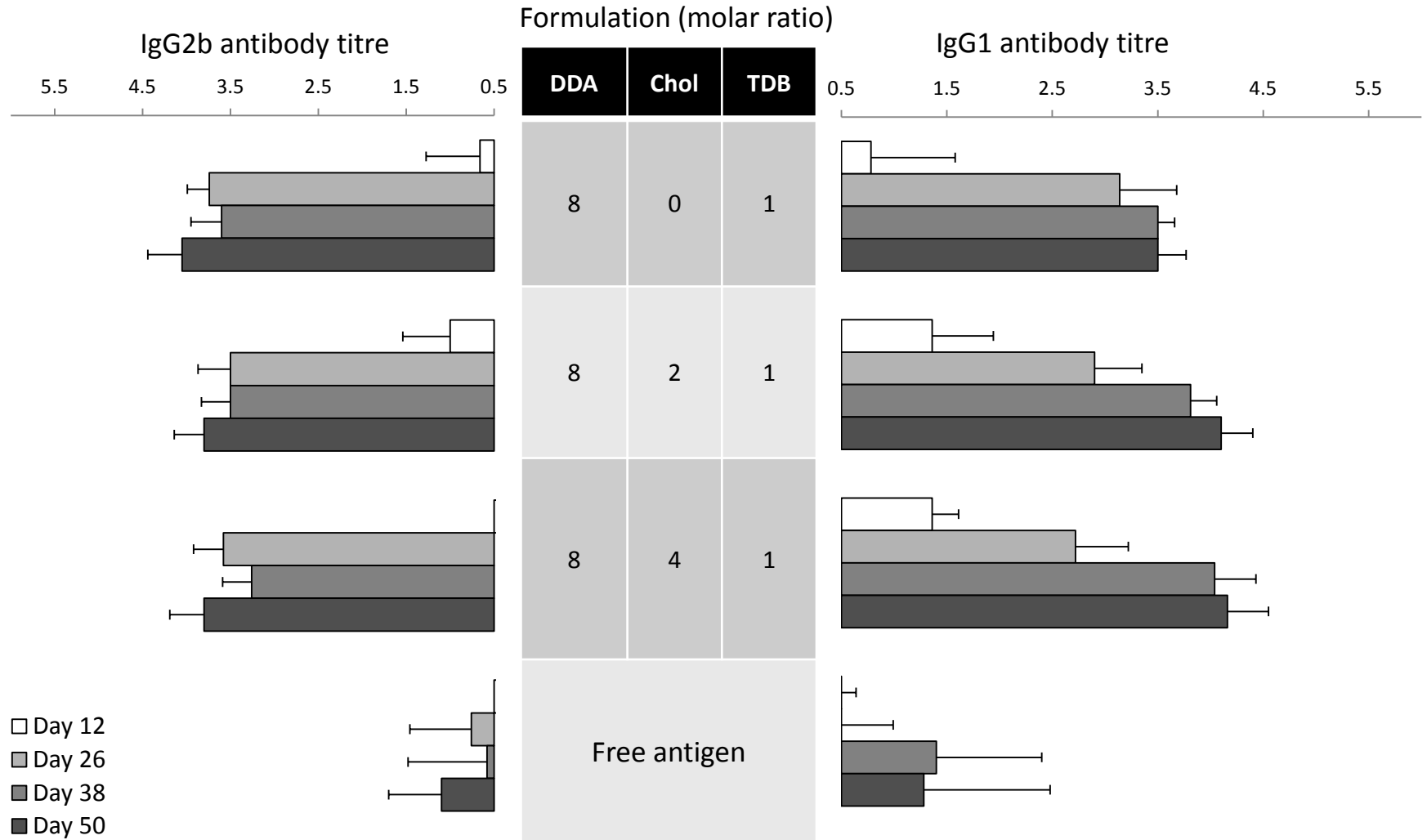


Figure 2B

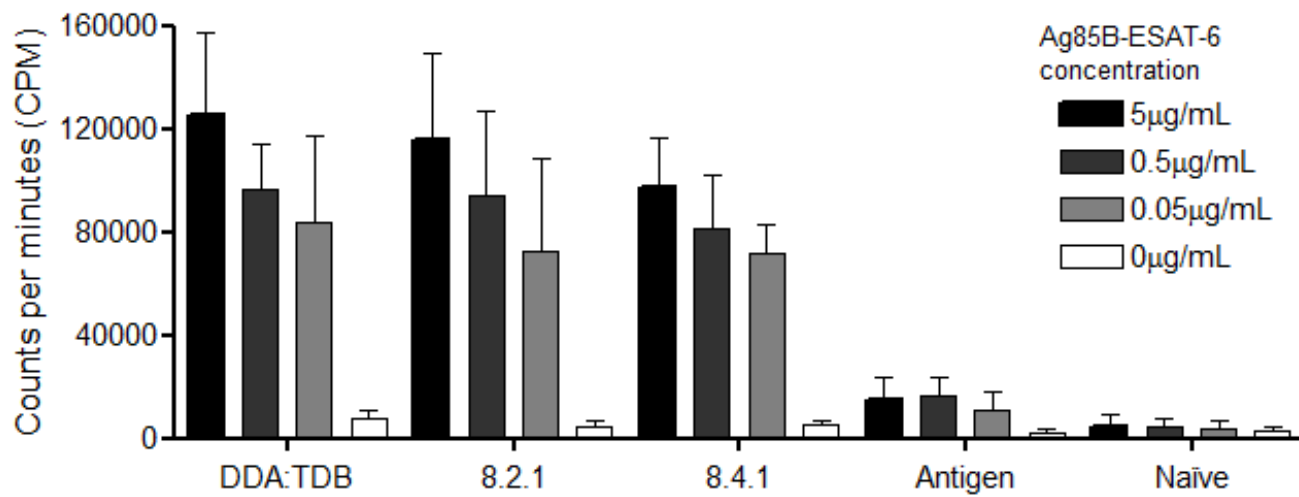


Figure 3.

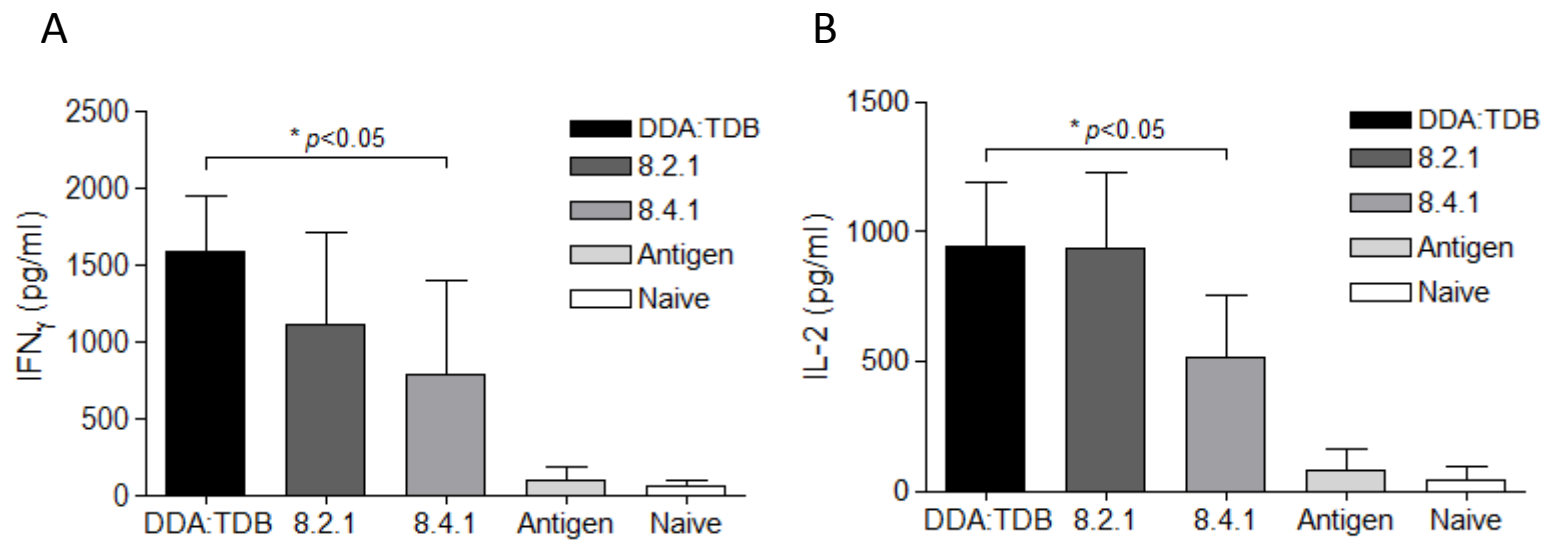


Figure 4.

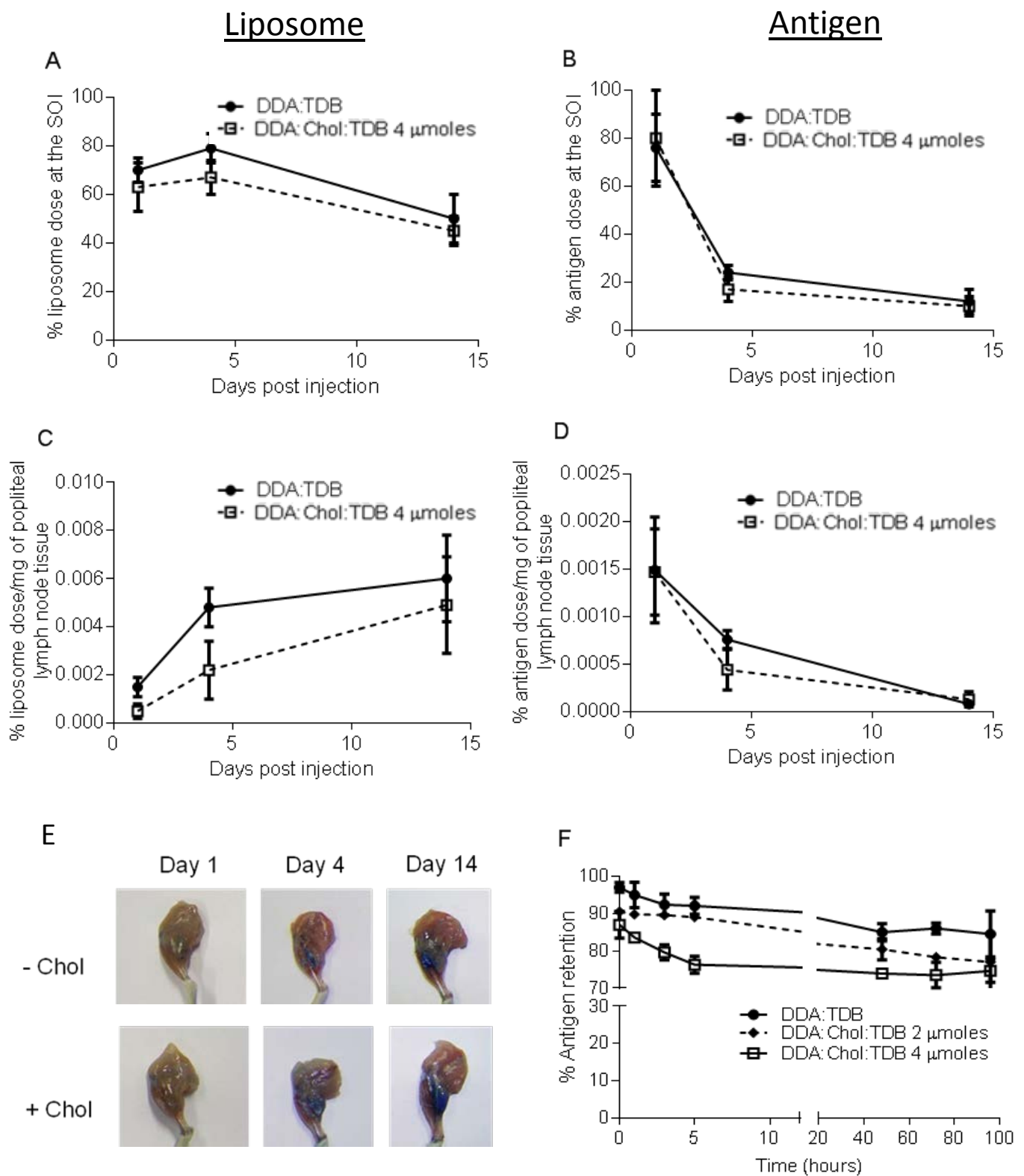


Figure 5.

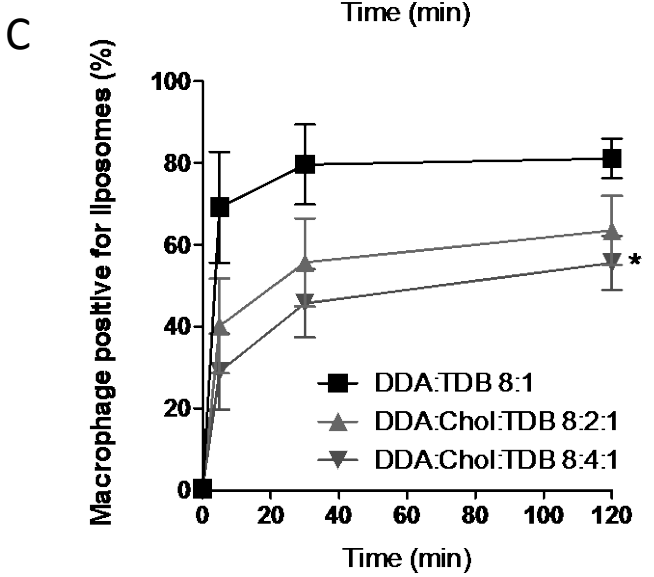
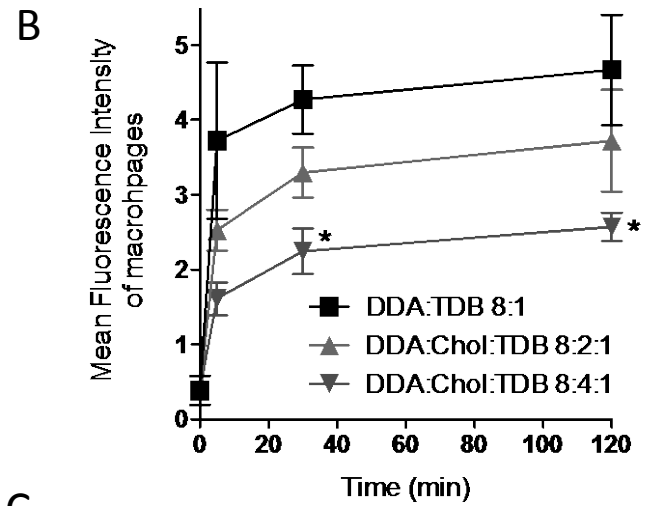
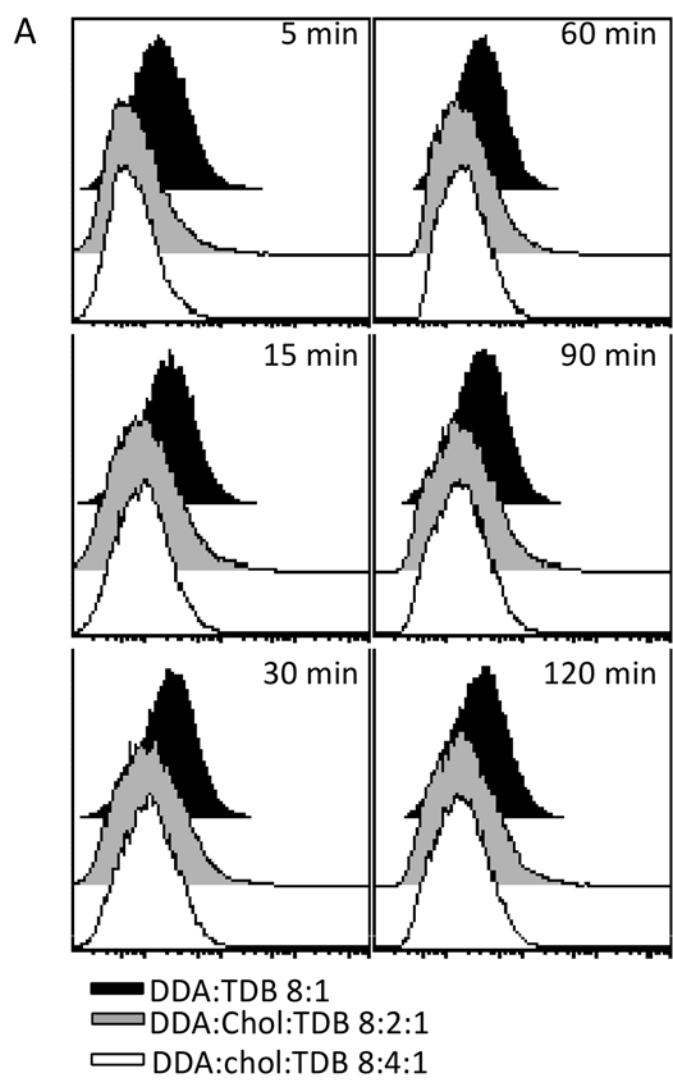


Figure 6.